

Flutter Margin Evaluation for Discrete-Time Systems

Hiroshi Torii*

Meijo University, Nagoya 468-8502, Japan
and

Yuji Matsuzaki†

Nagoya University, Nagoya 464-8603, Japan

A flutter prediction method using a new parameter is proposed, and its effectiveness is examined by numerical and experimental analysis. In this method, the aeroelastic system is identified as the autoregressive moving average (ARMA) model from the random response of a wing excited by flow turbulence, so that no special excitation device is needed. The new parameter is based on a stability test for discrete-time systems and is calculated algebraically from the autoregressive coefficients of the estimated ARMA model. Numerical calculation using a two-dimensional wing model shows that the parameter decreases almost linearly toward zero with increasing dynamic pressure. This is a superior property as a flutter predictor in comparison with damping coefficients and the stability parameter used conventionally. The method is applied to supersonic wind-tunnel flutter test data to examine the validity in actual data analysis. The results obtained under different test conditions demonstrate the advantage of the present method for an accurate and reliable flutter prediction. Moreover, an analytical consideration reveals that the calculated values of the proposed parameter are nearly equal to that of the flutter margin introduced by Zimmerman and Weissenburger (Zimmerman, N. H., and Weissenburger, J. T., "Prediction of Flutter Onset Speed Based on Flight Testing at Subcritical Speeds," *Journal of Aircraft*, Vol. 1, No. 4, 1964, pp. 190–202).

Nomenclature

| | | |
|----------------|---|--|
| A_0-A_3 | = | coefficients of discrete-time characteristic equation |
| $C_{L\alpha}$ | = | lift curve slope |
| $e(k)$ | = | white noise |
| F | = | flutter margin |
| F_z | = | new flutter prediction parameter |
| f_i | = | frequency of the i th mode |
| M | = | Mach number |
| P_0-P_3 | = | coefficients of characteristic equation |
| q | = | dynamic pressure |
| q_F | = | dynamic pressure at flutter boundary |
| \hat{q}_F | = | predicted value of q_F |
| s | = | complex variable used in the continuous-time system |
| s_i | = | characteristic root of the i th mode |
| T | = | sampling interval |
| $y(k)$ | = | sampled response of a wing |
| $y(t)$ | = | response of a wing |
| z | = | complex variable used in the discrete-time system |
| | | $z^{-1}y(k) = y(k-1)$ |
| z_i | = | discrete-time characteristic root of the i th mode |
| η_i | = | damping coefficient of the i th mode |
| θ | = | vector of the autoregressive moving average coefficients |
| $\hat{\theta}$ | = | the maximum likelihood estimate of θ |

Superscript

* = complex conjugate

Introduction

BECAUSE flutter causes serious damage to an aircraft, flight flutter tests are conducted to confirm the flutter boundary speed

Presented as Paper 98-1724 at the 39th Structures, Structural Dynamics, and Materials Conference, Long Beach, CA, 20–23 April 1998; received 5 January 1999; revision received 7 August 2000; accepted for publication 10 August 2000. Copyright © 2000 by the American Institute of Aeronautics and Astronautics, Inc. All rights reserved.

* Associate Professor, Department of Business Management, Tempaku. Member AIAA.

† Professor, Department of Aerospace Engineering, Chikusa. Member AIAA.

at the final stage of the development process. The tests are generally conducted at subcritical speeds to avoid structural damage, and so the flutter speed has to be predicted from the behavior of some stability criterion estimated against the flight speed or dynamic pressure. Therefore, it is quite significant for a reliable flutter prediction criterion to estimate the stability boundaries as accurately as possible.

Conventionally, the damping ratio of the critical mode has been used as the most common index of a flutter stability margin, and a lot of work has been directed to the accurate evaluation of modal damping.^{1–4} However, the estimation of modal damping is so sensitive to noise and error that it is difficult to obtain accurate and reliable data from flight tests. Furthermore, for an explosive type of flutter, the damping parameter shows no sign of instability up to the neighborhood of the critical speed. Thus, it is important to obtain a more suitable parameter for a better flutter prediction. In line with such a viewpoint, Zimmerman and Weissenburger⁵ introduced an alternative parameter called flutter margin, which is based on Routh's stability test and calculated using frequencies and modal dampings of coupling modes evaluated for a binary flutter case. The flutter margin decreases much more gradually with the increase of dynamic pressure than the damping of the critical mode. The analytical consideration using a bending-torsion wing model with quasi-steady aerodynamics shows that the flutter margin is expressed as a quadratic function of dynamic pressure. These are quite advantageous properties for the flutter prediction. Price and Lee⁶ have attempted the extension to trinary flutter.

Currently, measurement and analysis of test data are generally performed on a digital computer, where sampled data are processed to define the characteristics of the systems. System identification gives powerful and useful procedures to construct a linear discrete-time model, known as an autoregressive moving average (ARMA) model, from a random response of a wing excited by flow turbulence. Therefore, no special device of impulsive or sinusoidal excitation is needed in the flutter testing. The ARMA model consists of autoregressive (AR) terms of measurement, that is, a linear combination of the present and the finite number of past data, and the moving average (MA) of white noise. The AR part corresponds to the characteristic polynomial of the system and gives information on stability.

As a suitable approach for using with system identification procedures, Matsuzaki and Ando⁷ proposed a stability parameter method,

where a new flutter prediction index called a stability parameter is introduced. The stability parameter is based on Jury's⁸ stability analysis for the discrete-time system and is calculated algebraically from the identified AR coefficients. We have shown that the stability parameter is a more effective index for the flutter prediction than modal damping through numerical and experimental studies.^{7,9-11} Furthermore, the possibility of the real-time evaluation of the stability parameter for nonstationary systems is demonstrated in conjunction with recursive identification techniques.¹² However, with the increase of dynamic pressure, the stability parameter does not show gradual variation as the flutter margin does.

In this paper, a new flutter prediction parameter effectively applicable to the model obtained by system identification and having superior characteristics to the existing parameters is proposed. Analytical considerations are performed to obtain the relationship between the new parameter and dynamic pressure. At first, numerical analysis on a two-dimensional wing is performed to examine the behavior of the parameter and to show the advantage of the parameter in comparison with the modal damping and the stability parameter. Next, the present method is applied to supersonic wind-tunnel flutter test data to check its validity in a practical situation. The estimation of the parameter is conducted under different settings, and the results are compared with existing methods.

Flutter Prediction Method

In this section, a new flutter prediction method is proposed. The method consists of two parts: 1) identification of the aeroelastic system with an ARMA model from sampled data and 2) calculation of the flutter prediction parameter using the estimated AR coefficients. Only a binary flutter case is considered here. Therefore, the dynamics are expressed by the fourth-order characteristic equation.

Identification of System Dynamics

Because a wing is continuously excited by the turbulence of an airstream, the response of the wing $y(t)$ can be regarded as a random vibration. Therefore, data sampled at a constant interval T , $\{y(kT), k = 1, 2, \dots, N\}$, are considered to be a sequence of random variables. In the following, $\{y(kT)\}$ is written simply as $\{y(k)\}$. In system identification a random sequence is considered to be described by an AR or an ARMA model. In this study the sampled data $\{y(k)\}$ is identified with an ARMA model:

$$\alpha(z^{-1})y(k) = \beta(z^{-1})e(k) \quad (1)$$

where

$$\alpha(z^{-1}) = 1 + \alpha_1 z^{-1} + \dots + \alpha_n z^{-n}$$

$$\beta(z^{-1}) = 1 + \beta_1 z^{-1} + \dots + \beta_m z^{-m}$$

In the following, the ARMA model in which the order of $\alpha(z^{-1})$ and $\beta(z^{-1})$ are n and m , respectively, is denoted as ARMA(n, m). Here, the coefficients $\theta = \{\alpha_1, \dots, \alpha_n, \beta_1, \dots, \beta_m\}$, and the order n and m are unknown and are to be determined from $\{y(k)\}$.

The estimation of θ is obtained by

$$\hat{\theta} = \arg \max_{\theta} L(\theta) \quad (2)$$

where

$$L(\theta) = \frac{1}{(\sqrt{2\pi}\sigma)^N} \exp \left\{ -\frac{1}{2\sigma^2} \sum_{k=1}^N \left[\frac{\alpha(z^{-1})}{\beta(z^{-1})} y(k) \right]^2 \right\}$$

is a likelihood function. This is known as the maximum likelihood (ML) method.¹³ The maximization of $L(\theta)$ in Eq. (2) is iteratively evaluated. To determine the best order of the ARMA model, the Akaike's information criterion (AIC)

$$\text{AIC} = -2 \log[L(\hat{\theta})] + 2(n + m + 1) \quad (3)$$

is evaluated, and the combination of n and m that gives a minimum AIC is desirable.

Equation (1) means that the current value of $y(k)$ consists of the linear combination of the finite number of earlier measurements and a white noise sequence as external forces. The AR part, the left-hand side of Eq. (1), therefore, expresses the system dynamics and corresponds to the following characteristic polynomial in the discrete-time domain:

$$G(z) = z^n + \alpha_1 z^{n-1} + \dots + \alpha_{n-1} z + \alpha_n \quad (4)$$

As mentioned, the order of Eq. (1) should be determined by the AIC, but for the data that include M vibration modes, the order of the AR part should be set to $n = 2M$. Here, the extra frequency is filtered out to include only the two coupling modes that cause flutter. In the present case, a fourth-order characteristic polynomial

$$G(z) = z^4 + \alpha_1 z^3 + \alpha_2 z^2 + \alpha_3 z + \alpha_4 \quad (5)$$

should be estimated.

New Flutter Prediction Parameter

As a result of the ML estimation, the system dynamics related to flutter is expressed by Eq. (5). Here we rewrite Eq. (5) as follows:

$$\begin{aligned} G(z) &= A_4 z^4 + A_3 z^3 + A_2 z^2 + A_1 z + A_0 \\ &= A_4(z - z_1)(z - z_2)(z - z_3)(z - z_4), \quad A_4 > 0 \end{aligned} \quad (6)$$

where $z_3 = z_1^*$ and $z_4 = z_2^*$.

The stability of the discrete-time systems can be checked by the absolute value of the characteristic roots, that is, the stability condition of the system is that all of the characteristic roots are located within a unit circle in the Gauss plane (Fig. 1). If the characteristic polynomial is known, however, the stability can be verified from the coefficients without solving the characteristic roots. Jury's determinant method⁸ is one such stability test and is given in the Appendix.

By the application of Jury's method to Eq. (6), the system is stable if and only if all of the following conditions are satisfied:

$$G(1) = A_4 + A_3 + A_2 + A_1 + A_0 > 0 \quad (7)$$

$$G(-1) = A_4 - A_3 + A_2 - A_1 + A_0 > 0 \quad (8)$$

$$F^+(1) = A_4 + A_0 > 0 \quad (9)$$

$$F^-(1) = A_4 - A_0 > 0 \quad (10)$$

$$F^+(3) = \det(X_3 + Y_3) > 0 \quad (11)$$

$$F^-(3) = \det(X_3 - Y_3) > 0 \quad (12)$$

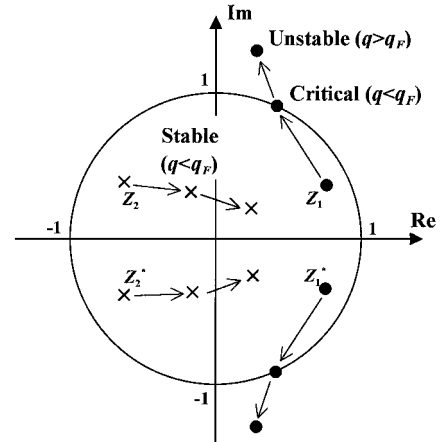


Fig. 1 Typical loci of characteristic roots.

where

$$X_3 = \begin{bmatrix} A_4 & A_3 & A_2 \\ 0 & A_4 & A_3 \\ 0 & 0 & A_4 \end{bmatrix}, \quad Y_3 = \begin{bmatrix} A_2 & A_1 & A_0 \\ A_1 & A_0 & 0 \\ A_1 & 0 & 0 \end{bmatrix}$$

The aeroelastic system is stable at low speeds and becomes unstable due to flutter at a certain higher speed. At the flutter speed one of the parameters (7–12) becomes zero. The important point is which parameter among them is critical for flutter. Because $F^-(n-1)$ for an n th order system is expanded using the characteristic roots as Eq. (A6) in the Appendix, the corresponding parameter $F^-(3)$ for the present case can be expressed by

$$F^-(3) = A_4^3 \prod_{\substack{i,j=1 \\ i < j}}^4 (1 - z_i z_j) \\ = A_4^3 |1 - z_1 z_2|^2 |1 - z_1 z_3|^2 (1 - |z_1|^2) (1 - |z_2|^2) \quad (13)$$

This means that $F^-(3)$ becomes zero at the flutter boundary, where either $|z_1| = 1$ or $|z_2| = 1$ is satisfied, because the third or fourth factor of the last equation becomes zero. Consequently, $F^-(3)$ can be used as the flutter predictor. It is also true for the system of more than two modes that $F^-(n-1)$ gets to zero at the flutter speed. In the stability parameter method,⁷ $F^-(n-1)$ is called the stability parameter and is utilized for the flutter prediction.

Though the stability parameter is a better index for flutter prediction than the modal damping, its behavior against dynamic pressure is inferior to the flutter margin. To overcome this drawback, the authors propose the use of a new flutter prediction parameter defined by

$$F_z = \frac{F^-(3)}{F^-(1)^2} = \frac{\det(X - Y)}{(A_4 - A_0)^2} \quad (14)$$

This is applicable for two-mode systems.

Note that Eq. (14) has no singularity in $q \leq q_F$. Because $F^-(1)$ is expressed as

$$F^-(1) = A_4 (1 - |z_1|^2 |z_2|^2) \quad (15)$$

and the loci of roots are depicted schematically in Fig. 1, it is obvious that $F^-(1) > 0$ for $q < q_F$ because both $|z_1|$ and $|z_2|$ are less than 1. At $q = q_F$, except for the improbable case in which both modes become critical simultaneously, a pair of roots reaches on a unit circle ($|z_1| = 1$) and another pair is still located within a unit circle ($|z_2| < 1$) so that $F^-(1) > 0$. Therefore, $F^-(1) > 0$ for $q \leq q_F$, that is, the denominator of Eq. (14) does not become zero.

Because the numerator of Eq. (11) is the stability parameter $F^-(3)$, F_z has the following property:

$$\begin{cases} F_z > 0 & \text{for } q < q_F \\ F_z = 0 & \text{for } q = q_F \end{cases}$$

The flutter boundary is predicted as the dynamic pressure at which F_z becomes zero.

Analytical Consideration

For a bending-torsion model with quasi-steady aerodynamics, the flutter margin F is expressed as a quadratic function of dynamic pressure⁵:

$$F = C_2 (C_{L\alpha} q)^2 + C_1 (C_{L\alpha} q) + C_0 \quad (16)$$

This is an outstanding property that the other parameters used for predicting the flutter boundary do not have. In this section, an analytical consideration for the new parameter F_z is attempted to obtain the basic properties and the relationship with dynamic pressure.

Suppose that the characteristic equation of a two-degree-of-freedom system is given by

$$s^4 + P_3 s^3 + P_2 s^2 + P_1 s + P_0 = 0 \quad (17)$$

The exact transform between the continuous- and the discrete-time system for the property of F_z in conjunction with Eq. (17) is too complicated to consider. Hence, we use the Tustin transformation (see Ref. 14),

$$s^n = \{(2/T)[(z-1)/(z+1)]\}^n \quad (18)$$

which is an easy and simple method used to obtain the counterpart expression of a continuous-time system approximately. Then the approximate discrete-time characteristic equation is expressed by

$$A_4 z^4 + A_3 z^3 + A_2 z^2 + A_1 z + A_0 = 0 \quad (19)$$

where

$$A_4 = 1 + P_3(T/2) + P_2(T/2)^2 + P_1(T/2)^3 + P_0(T/2)^4 \quad (20)$$

$$A_3 = -4 - 2P_3(T/2) + 2P_1(T/2)^3 + 4P_0(T/2)^4 \quad (21)$$

$$A_2 = 6 - 2P_2(T/2)^2 + 6P_0(T/2)^4 \quad (22)$$

$$A_1 = -4 + 2P_3(T/2) - 2P_1(T/2)^3 + 4P_0(T/2)^4 \quad (23)$$

$$A_0 = 1 - P_3(T/2) + P_2(T/2)^2 - P_1(T/2)^3 + P_0(T/2)^4 \quad (24)$$

By the substituting of Eqs. (20–24) into Eq. (14), F_z is expressed as

$$F_z \approx \frac{T^4 (-P_1^2 + P_1 P_2 P_3 - P_0 P_3^2)}{[P_3 + P_1(T/2)^2]^2} \quad (25)$$

If the sampling interval T is small, the higher-order terms of T are negligible. Hence, Eq. (25) is approximated by

$$F_z \approx T^4 [-(P_1/P_3)^2 + P_2(P_1/P_3) - P_0] \quad (26)$$

The flutter margin for Eq. (17) is defined by

$$F = -(P_1/P_3)^2 + P_2(P_1/P_3) - P_0 \quad (27)$$

Hence, Eq. (26) means

$$F_z \approx T^4 F \quad (28)$$

that is, F_z is nearly equal to the flutter margin except for the constant multiplier. For the same model used in Ref. 5, therefore, F_z can be approximated by a quadratic function of q :

$$F_z \approx T^4 [C_2 (C_{L\alpha} q)^2 + C_1 (C_{L\alpha} q) + C_0] \quad (29)$$

Because some approximations are introduced to derive Eq. (28), it is not possible for F_z to be equal to the flutter margin. However, F_z is expected to behave in a similar manner to that of the flutter margin.

Comparison with Existing Methods

In this section, the more realistic behavior of F_z is studied using numerical analysis of a bending-torsion wing (Fig. 2) with unsteady incompressible aerodynamics and is compared with the modal damping η_1 and the stability parameter $F^-(3)$. The configuration of the wing model is the same as in Ref. 10: $\omega_h = 50$ rad/s, $\omega_a = 100$ rad/s, $\alpha = -0.4$, and $x_a = 0.2$. An aerodynamic pressure load is derived from Theodorsen's theory. Eigenvalue analysis for the resulting equations of motion gives the characteristic roots of this aeroelastic system.

Suppose that the characteristic roots of two dynamic modes are described by s_i , $i = 1, 2$. Then the modal damping values are calculated by

$$\eta_i = -(\text{Re } s_i / |s_i|) \quad (30)$$

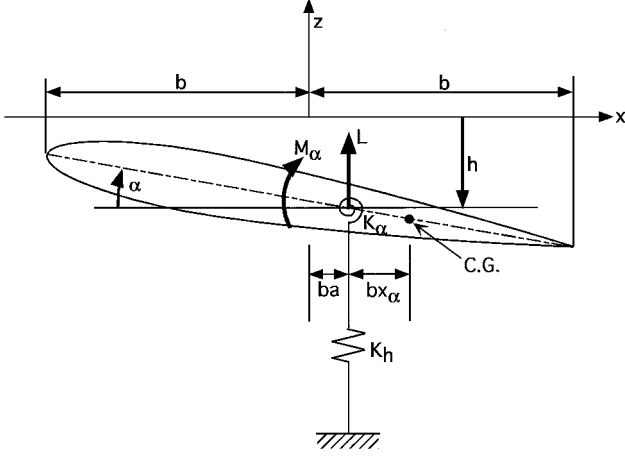


Fig. 2 Two-dimensional wing model.

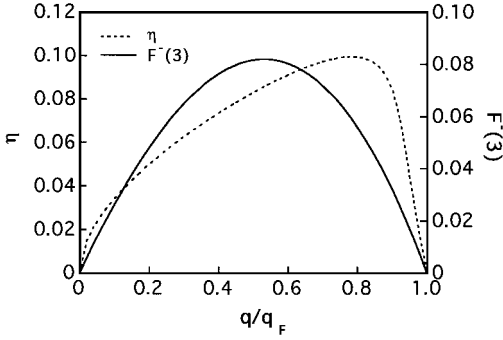


Fig. 3 Modal damping and stability parameter of the two-dimensional wing model.

The characteristic polynomial in the discrete-time domain is obtained by

$$G(z) = \prod_{i=1}^2 (z - z_i)(z - z_i^*) = A_4 z^4 + A_3 z^3 + A_2 z^2 + A_1 z + A_0, \quad A_4 = 1 \quad (31)$$

where z_i is the discrete-time characteristic root that is transformed by

$$z_i = \exp(s_i T) \quad (32)$$

Here the sampling interval was set to $T = 0.01$ s. The stability parameter $F^-(3)$ and the present parameter F_z are evaluated from the coefficients of Eq. (31). The modal damping is also calculated from z_i by

$$\eta_i = -(\ln|z_i|/|\ln z_i|) \quad (33)$$

which gives the same value as Eq. (30).

Figure 3 shows the value of η_1 and $F^-(3)$ plotted against normalized dynamic pressure q/q_F . The damping η_1 increases up to $q/q_F = 0.8$ and then starts to decrease rapidly toward zero, whereas $F^-(3)$ starts to decrease at around $q/q_F = 0.5$. This means that the flutter tests should be conducted in the range of $q/q_F > 0.8$ for η_1 and $q/q_F > 0.5$ for $F^-(3)$.

As shown in Fig. 4, the parameter F_z decreases almost linearly in the entire subcritical dynamic pressure and is obviously a more effective index for the flutter prediction than η_1 and $F^-(3)$ described in Fig. 3. This result suggests that a linear fitting for F_z gives a reasonable prediction of the flutter boundary, though F_z was shown to be approximated by a quadratic equation in the preceding section.

For reference, the flutter margin was evaluated by Eq. (27) using the characteristic polynomial:

$$G(s) = \prod_{i=1}^2 (s - s_i)(s - s_i^*) = s^4 + P_3 s^3 + P_2 s^2 + P_1 s + P_0 \quad (34)$$

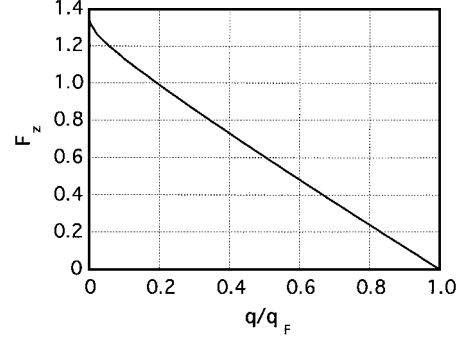
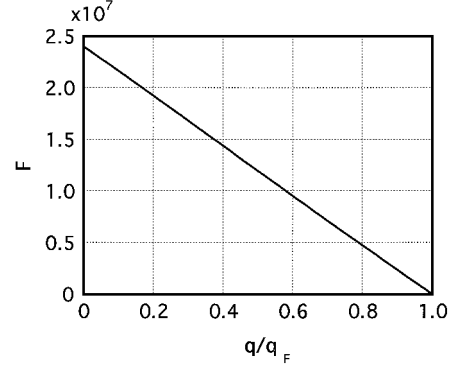
Fig. 4 Parameter F_z of the two-dimensional wing model.

Fig. 5 Flutter margin of the two-dimensional wing model.

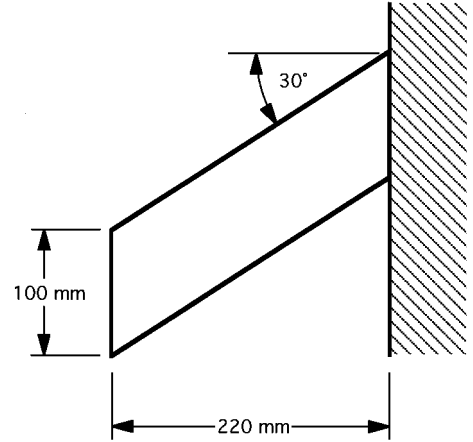


Fig. 6 Planform of the swept-back wing model.

and is depicted in Fig. 5. When compared to Fig. 4, it is clear that the behavior of F_z is quite similar to that of the flutter margin F . The order of the ratio F_z to F is

$$O(F_z/F) \approx 10^{-8}$$

which coincides with the order of T^4 as expressed in Eq. (28).

Application to Wind-Tunnel Experiment

To ascertain the practical applicability of the proposed method, the supersonic wind-tunnel flutter testing data were analyzed. Figure 6 illustrates the planform of a swept-back wing model, which is made of aluminum alloy flat plate of 2-mm thickness. The response was measured by strain gauges attached on both sides of the wing. The Mach number was fixed at $M = 2.51$ for all tests. The stationary tests were conducted at 11 dynamic pressures from $q = 75.7$ to 99.4 kPa. A sampling interval T was set to 2 ms. The number of data used for parameter estimation was $N = 6000$. According to the AIC, ARMA(4,3) was selected as the model to be identified. Flutter occurs due to the coupling of the first and second modes.

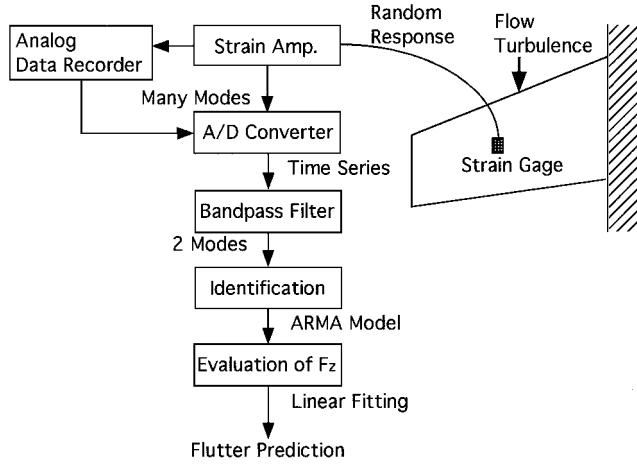


Fig. 7 Flowchart of flutter prediction.

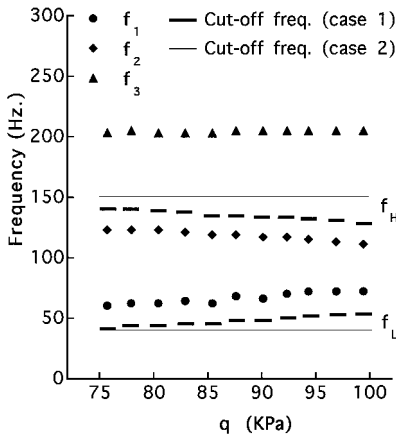


Fig. 8 Modal frequencies of the lowest three modes and cutoff frequencies of filter.

Figure 7 describes the flow of data processing. The signal measured on the wing is digitized to be a time series by an A/D converter. The digital data are then processed to eliminate low-frequency noise and higher modes using a digital filter. As a result of filtering, the data include only the lowest two modes. Then the data are identified with the ARMA model, in which the coefficients are estimated by the ML method. Here, the MATLAB® System Identification Toolbox is used to estimate the ARMA coefficients. The flutter boundary is predicted by a linear fitting to F_z as evaluated. According to Eq. (29), F_z should be fitted by a quadratic curve, but there is a possibility of giving a meaningless prediction when the range of q is not wide enough to obtain a quadratic equation. On the other hand, as shown in Fig. 4, the curve of F_z against q is almost linear. Therefore, a linear fit is considered to be reasonable for the present case.

The setting of a filter influences the estimation of the parameters as well as the choice of sampling interval and model structure. Generally, the adjustment of such conditions is very important to obtain an accurate estimation. As a first case of the analysis, the bandwidth of a filter was adjusted adaptively according to the modal frequencies, that is, the cutoff frequencies of the lower and the higher bound were set to

$$f_L = f_1 - 16.5, \quad f_H = f_2 + 16.5$$

given in hertz, where f_1 and f_2 are the first and second modal frequencies estimated at each dynamic pressure. These are the same settings used in Ref. 9. The lowest three modal frequencies and the cutoff frequencies are depicted in Fig. 8. Figures 9–11 describe the estimated results of the modal dampings η_1 and η_2 , the stability parameter $F^-(3)$, and the parameter F_z , respectively. The symbol \times indicates the actual flutter boundary, $q_F = 113.5$ kPa, observed experimentally. As shown in Fig. 9, the modal damping

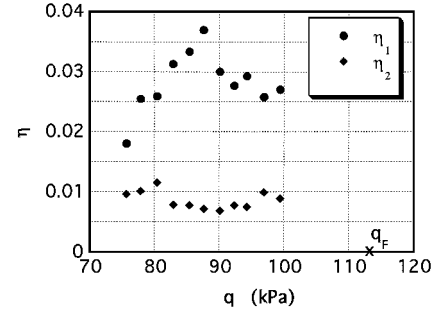


Fig. 9 Estimation results of η_1 and η_2 using a filter with adjusted bandwidth; $[f_L, f_H] = [f_1 - 16.5, f_2 + 16.5]$, hertz.

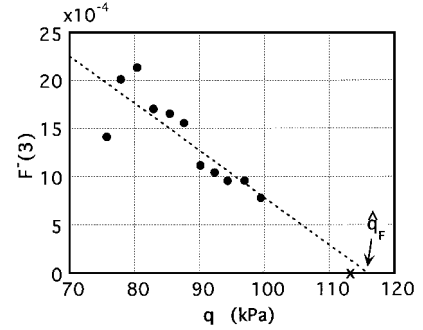


Fig. 10 Estimation results of $F^-(3)$ using a filter with adjusted bandwidth; $[f_L, f_H] = [f_1 - 16.5, f_2 + 16.5]$, hertz.

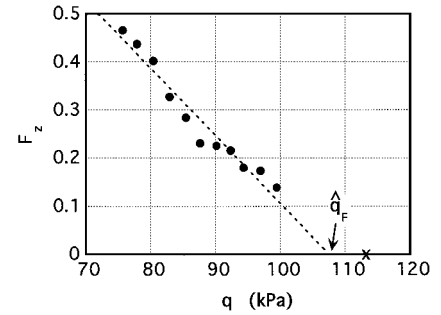


Fig. 11 Estimation results of F_z using a filter with adjusted bandwidth; $[f_L, f_H] = [f_1 - 16.5, f_2 + 16.5]$, hertz.

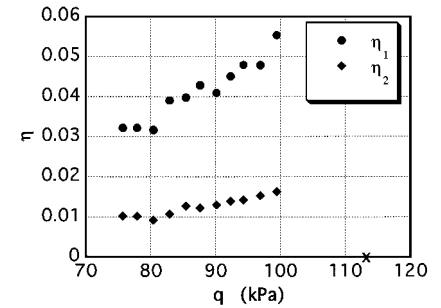


Fig. 12 Estimation results of η_1 and η_2 using a filter with fixed bandwidth; $[f_L, f_H] = [40, 150]$, hertz.

gives no useful information on the critical dynamic pressure. On the other hand, Figs. 10 and 11 show that $F^-(3)$ and F_z decrease monotonously toward zero with increasing dynamic pressure. The critical dynamic pressures predicted by a linear fitting to $F^-(3)$ and F_z were $\hat{q}_F = 116.2$ kPa (error = +2%) and $\hat{q}_F = 108.5$ kPa (error = -4%), respectively.

In an online data analysis, the best setting of a filter is unknown in advance. As a second case, therefore, the cutoff frequencies of the bandpass filter were fixed to $f_L = 40$ and $f_H = 150$ Hz for all analyses. Figures 12 and 13 show that the results of both η_i and

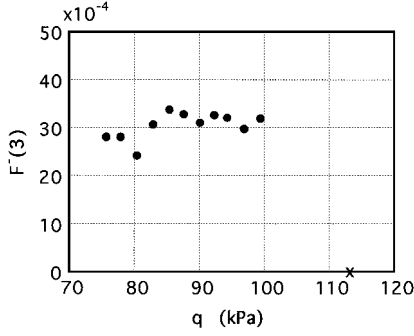


Fig. 13 Estimation results of $F^-(3)$ using a filter with fixed bandwidth; $[f_L, f_H] = [40, 150]$, hertz.

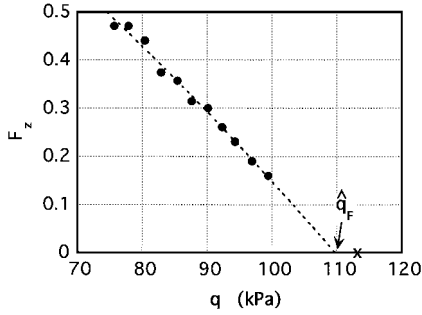


Fig. 14 Estimation results of F_z using a filter with fixed bandwidth; $[f_L, f_H] = [40, 150]$, hertz.

$F^-(3)$ are quite different than those of the earlier cases and do not give a respectable prediction of flutter under this condition. These parameters are very sensitive to the change of filter setting. As shown in Fig. 14, however, the estimated values of F_z are similar to the earlier result depicted in Fig. 11. On a linear fitting, F_z gives the flutter prediction of $\hat{q}_F = 110.0$ kPa (error = -3%).

Conclusions

The authors proposed a new flutter prediction parameter F_z , which is defined for discrete-time systems and is convenient for coping with system identification algorithms. An analytical consideration showed that the calculated values of F_z are nearly equal to that of the flutter margin introduced by Zimmerman and Weissenburger⁵ and were expressed as a quadratic function of the dynamic pressure for a bending-torsion wing model with quasi-steady aerodynamics. The numerical analysis of a wing with unsteady incompressible aerodynamic forces showed that F_z varied almost linearly toward zero with the increase of dynamic pressure in the whole subcritical range, which is similar in behavior to the flutter margin, whereas the damping coefficient and the stability parameter start to decrease at around 80 and 50%, respectively, of the flutter boundary dynamic pressure. Therefore, F_z is advantageous for an effective and reliable flutter prediction compared with modal damping and the stability parameter. The application to supersonic wind-tunnel flutter testing data showed that the present method gave an accurate and reliable flutter prediction regardless of the filter setting, which had a great influence on the estimation of the modal dampings and the stability parameter.

In the present definition, the parameter F_z is not applicable for more than two modes, and so the stability parameter $F^-(2M-1)$ should be used for M -modes systems ($M > 2$). However, if all but a couple of modes that cause flutter can be eliminated by a bandpass and a bandstop filter, this method will be applicable to such systems.

Appendix: Jury's Determinant Method

A discrete-time system is stable if and only if all of the characteristic roots are located inside a unit circle in the Gauss plane. Jury's determinant method⁸ judges the stability of a discrete-time system based on the characteristic polynomial without solving the roots.

Suppose that the characteristic equation of the discrete-time system is given by

$$G(z) = A_n z^n + A_{n-1} z^{n-1} + \cdots + A_1 z + A_0 \quad (A1)$$

where n is an even number. Then the necessary and sufficient conditions that the system is stable are that all of the following parameters are positive:

$$G(1) = A_n + A_{n-1} + \cdots + A_1 + A_0 \quad (A2)$$

$$G(-1) = A_n - A_{n-1} + \cdots - A_1 + A_0 \quad (A3)$$

$$F^+(k) = \det(X_k + Y_k) \quad (k = 1, 3, \dots, n-1) \quad (A4)$$

$$F^-(k) = \det(X_k - Y_k) \quad (k = 1, 3, \dots, n-1) \quad (A5)$$

where X_k and Y_k are $k \times k$ matrices whose elements consist of the coefficients of Eq. (A1):

$$X_k = \begin{bmatrix} A_n & \cdots & A_{n-k+1} \\ 0 & \ddots & \vdots \\ 0 & 0 & A_n \end{bmatrix}, \quad Y_k = \begin{bmatrix} A_{k-1} & \cdots & A_0 \\ \vdots & \ddots & 0 \\ A_0 & 0 & 0 \end{bmatrix}$$

Among these parameters, $F^-(n-1)$ can be expressed by means of characteristic roots as follows¹⁵:

$$F^-(n-1) = A_n^{n-1} \prod_{i < j} (1 - z_i z_j) \quad (A6)$$

Therefore, $F^-(n-1)$ becomes zero whenever any pair of complex conjugate characteristic roots reaches a unit circle, that is, the stability boundary.

Acknowledgments

The National Aerospace Laboratory (NAL) provided the flutter test data used in this work. The authors wish to thank the NAL and Yasukatsu Ando for his help and useful advice.

References

- Kordes, E. E. (ed.), "Flutter Testing Techniques," NASA SP-415, Oct. 1975.
- Walker, R., and Gupta, N., "Real-Time Flutter Analysis," NASA CR-170412, March 1984.
- Roy, R., and Walker, R., "Real-Time Flutter Identification," NASA CR-3933, Oct. 1985.
- Lee, B. H. K., and Laichi, F., "Development of Post-Flight and Real Time Flutter Analysis Methodologies," Actes Forum International Aeroelasticite et Dynamique de Structures, Strasbourg, France, May 1993.
- Zimmerman, N. H., and Weissenburger, J. T., "Prediction of Flutter Onset Speed Based on Flight Testing at Subcritical Speeds," *Journal of Aircraft*, Vol. 1, No. 4, 1964, pp. 190-202.
- Price, S. J., and Lee, B. H. K., "Evaluation and Extension of the Flutter-Margin Method for Flight Flutter Prediction," *Journal of Aircraft*, Vol. 30, No. 3, 1993, pp. 395-402.
- Matsuzaki, Y., and Ando, Y., "Estimation of Flutter Boundary from Random Responses Due to Turbulence at Subcritical Speeds," *Journal of Aircraft*, Vol. 18, No. 10, 1981, pp. 862-868.
- Jury, I. E., *Theory and Application of the z-Transform Method*, Wiley, New York, 1964, pp. 136-139.
- Matsuzaki, Y., and Ando, Y., "Flutter and Divergence Boundary Prediction from Nonstationary Random Responses at Increasing Flow Speed," AIAA Paper 85-0691, 1985.
- Matsuzaki, Y., and Torii, H., "Response Characteristics of a Two-Dimensional Wing Subject to Turbulence Near the Flutter Boundary," *Journal of Sound and Vibration*, Vol. 136, No. 2, 1990, pp. 187-199.
- Torii, H., and Matsuzaki, Y., "Subcritical Flutter Characteristics of a Swept-Back Wing in a Turbulent Supersonic Flow: Comparison Between Analysis and Experiment," AIAA Paper 92-2393, 1992.
- Torii, H., and Matsuzaki, Y., "Flutter Boundary Prediction Based on Nonstationary Data Measurement," *Journal of Aircraft*, Vol. 34, No. 3, 1997, pp. 427-432.
- Ljung, L., *System Identification—Theory for the User*, Prentice-Hall, Englewood Cliffs, NJ, 1987, pp. 181-190.
- Houpis, C. H., and Lamont, G. B., *Digital Control Systems—Theory, Hardware, Software*, McGraw-Hill, New York, 1985, pp. 234-256.
- Jury, I. E., and Pavlidis, T., "Stability and Aperiodicity Constraints for System Design," *IEEE Transactions on Circuit Theory*, Vol. 10, No. 1, 1963, pp. 137-141.